IET Image Processing

Research Article

IET Journals
The Institution of Engineering and Technology

Automated segmentation of the epidermis area in skin whole slide histopathological images

ISSN 1751-9659
Received on 26th March 2014
Revised on 23rd February 2015
Accepted on 14th March 2015
doi: 10.1049/iet-ipr.2014.0192
www.ietdl.org

Cheng Lu[1] ✉, *Zhen Ma*[2], *Mrinal Mandal*[3]

[1]*College of Computer Science, Shaanxi Normal University, Xi'an 710119, Shaanxi Province, People's Republic of China*
[2]*College of Food Engineering and Nutritional Science, Shaanxi Normal University, Xi'an 710119 Shaanxi Province, People's Republic of China*
[3]*Electrical and Computer Engineering, University of Alberta, Edmonton, Alberta, Canada T6G 2V4*
✉ *E-mail: chenglu@snnu.edu.cn*

Abstract: With the development of high-speed, high-resolution whole slide histology digital scanners, glass slides of tissue specimen can now be digitised at high magnification to create the whole slide image. Quantitative image analysis tools are then desirable to help the pathologist for their routine examination. Epidermis area is a very important observation area for the cancer diagnosis. Therefore, in order to build up a computer-aided diagnosis system, segmentation of the epidermis area is often the very first and crucial step. An improved computer-aided epidermis segmentation technique for the whole slide skin histopathological image is proposed in this study. The proposed technique first obtains an initial segmentation result with the help of global thresholding and shape analysis. A template matching method, with adaptive template intensity value, is then applied. Finally, a threshold is calculated based on the probability density function of the response value image. Experimental results show that the proposed technique overcomes the limitation of the existing technique and provides superior performance, with sensitivity of 95.68%, specificity of 99.41% and precision of 93.13%. The performance of the proposed technique is satisfactory for future clinical use.

1 Introduction

Histopathology slides provide a cellular-level view of the diseased tissue, and is considered the gold standard in the diagnosis of diseases for almost all kinds of cancer. Traditionally, histopathological slides are examined under a microscope by pathologists, who have been through long and intense pathology training. The diagnostic decisions are then made based on well-defined histological criterion combined with their personal experience. However, the decisions are subjective and often lead to intra-observer and inter-observer variability [1–3]. With the help of whole slide histology digital scanners, glass slides of tissue specimen can now be digitised at high magnification to create the whole slide image (WSI). Such high-resolution images are similar to what a pathologist observes under a microscope to diagnose the biopsy [4, 5]. However, quantitative analysis of digitised WSI is time-consuming and difficult. To address such limitations, computer-aided quantitative tools which can provide objective results are needed. Recently, researchers have applied sophisticated digital image analysis techniques to extract objective and accurate prognostic information throughout the WSI [6, 7]. Additionally, instead of accessing only representative regions, the computerised system can process the whole slide and prevent sampling bias.

Skin melanoma is the most aggressive type of skin cancer [8]. The early detection of malignant melanoma will help to lower the mortality rate. A normal skin tissue slide usually contains three main parts: epidermis area, dermis area and subcutaneous tissues (see Fig. 1, the bottom image shows the manually labelled epidermis area). When a pathologist examines a skin tissue, epidermis area is often the first target since it is a crucial observation area to be considered in the diagnosis procedure. Since the global/architectural and morphological features of atypia cells in the epidermis or epidermis–dermis junctional area are key factors to be considered in order to grade a skin tissue [9]. For example, the thickness of epidermis may provide diagnosis clue for cancer diagnosis. Another example is that the distribution of melanocytes is an important marker in melanoma diagnosis.

Several computerised techniques have been proposed for quantitative analysis of skin histopathological images. Lu and Mandal [10] proposed several image analysis techniques, which include the segmentation of epidermis area, segmentation of keratinocytes [11] and melanocytes [12, 13]. In reference [10], Lu and Mandal utilised a global threshold and shape analysis to segment the epidermis area in the red channel skin WSI (we refer this technique as EMBS technique hence forth). The EMBS technique has been evaluated on a set of 33 WSIs and obtains good performance in terms of sensitivity and specificity. However, the precision rate is relatively low since the segmentation result tends to include many false positive regions. Mokhtari *et al.* [5] proposed a similar epidermis segmentation technique based on contrast limit adaptive histogram equalisation (CLAHE). The CLAHE-based technique first performs morphological closing with a disk-shaped structuring element to remove the noise in image. The CLAHE is then used to adaptively adjust local contrast of the image. Finally, a global thresholding method is utilised to segment the epidermis area. To predict sentinel lymph node status of melanoma patients, *Nielsen et al.* [14] proposed to compute the melanoma antigen recognised by T cells-1 (MART1)-verified Ki-67 indices in epidermis and dermis. The automated quantifications show promising results in melanoma differentiation.

In this paper, we investigate the limitations of the existing epidermis segmentation techniques and propose an improved technique for automatic segmentation of the epidermis area in the skin WSI. The organisation of this paper is as follows. In Section 2, we discuss the proposed technique, followed by the performance evaluations in Section 3. The conclusion is presented in Section 4.

2 Proposed technique

The overall schematic of the proposed technique is presented in Fig. 2. The proposed technique contains three modules. Given a skin WSI, module one obtains an initial epidermis segmentation result with the help of global threshold combined with a shape

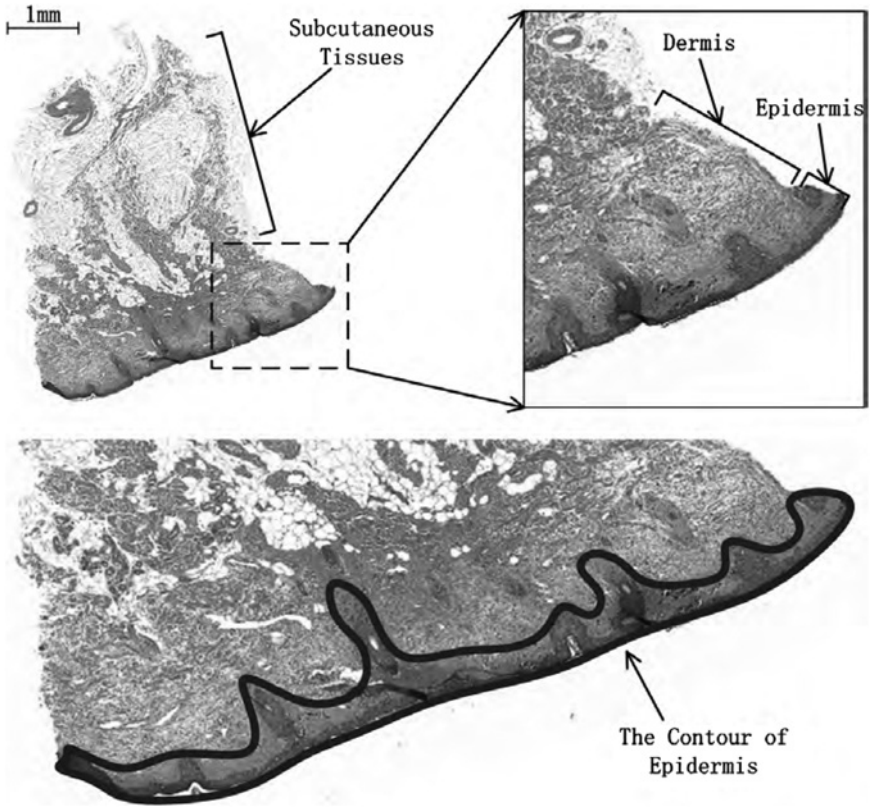

Fig. 1 *Anatomy of a skin tissue*

analysis method. In the second module, a template matching (TM) method with automated generated template is applied onto the pre-segmented rough epidermis area. A response value image is obtained. In the last module, the probability density function (PDF) of the response value image is analysed so that final segmentation result of the epidermis area is obtained. The details of these modules are discussed below.

2.1 Initial segmentation of epidermis

In this module, an initial segmentation of epidermis is obtained using a global threshold and shape analysis method [10]. Before the thresholding is performed, pixels with intensity >240 are removed, which correspond to the background pixels, to obtain more accurate result.

As discussed in our previous work [10], the red channel image provides the best discrimination between the dermis and epidermis. In this paper, all processings are performed on the red channel of the original red, green and blue image. Since the epidermis area has lower intensity value compared with the remaining part of a WSI (see Figs. 3*a* and *b*, where the lower part of the image contains epidermis), a simple threshold method is able to segment the epidermis and background. The threshold method divides the image pixels into two groups: foreground and background, based on the pixel intensity. Specifically, let τ be a selected threshold. The classification of pixel p with intensity value $g(p)$ is then calculated as follows

$$p = \begin{cases} \text{foreground}, & \text{if } g(p) \le \tau \\ \text{background}, & \text{if } g(p) > \tau \end{cases} \quad (1)$$

Fig. 2 *Schematic of the proposed technique*

In the set of epidermis segmentation, the foreground corresponds to the epidermis area. We utilise Otsu's thresholding [15] method to calculate a global threshold for segmentation.

Examples of the threshold result are shown in Figs. 3*b* and *e*. Note that other unrelated regions, such as hair follicles and blood vessels, are segmented, accompany with the epidermis areas. That is because such unrelated regions also have lower intensity value. If we label all the regions in the binary image via 8-connected criterion [16] and denote all such 8-connected regions as $\{\mathcal{C}_i\}_{i=1,\ldots,n}$, where n is the total number of the regions. It is expected that, in a typical image, several hundreds of 8-connected regions will still exist in the segmentation result. Therefore a further test is still required to eliminate the unrelated false positive regions.

To eliminate the false regions, we incorporate domain specific knowledge to eliminate the undesirable regions using the shape analysis on the binary image. Basically, two domain knowledge are applied for the shape analysis: size and shape of the regions. In terms of the size, it is known that the size of epidermis is greater than a predefined size threshold T_{area}. We set $T_{\text{area}} = \mathcal{N} \times T_{\text{pea}}$, where $\mathcal{N}$ is the total pixel number of digital skin image. T_{pea} is a fraction number, set $T_{\text{pea}} = 0.3$ to 0.6% empirically, which determined based on experimental tests and domain prior, and represents the weight of epidermis area in the WSI. In terms of the shape, it is expected that the epidermis area is a narrow and long region. We can quantify such shape feature by the ratio of major axis length (l_1) to minor axis length (l_2) of a best fit ellipse [17].

For each 8-connected region $\mathcal{C}_i$ in the binary image, we can now apply the above-mentioned criteria to distinguish the epidermis and other tissue components using the following equation

$$\mathcal{C}_i = \begin{cases} \text{epidermis}, & \text{if } A(\mathcal{C}_i) \ge T_{\text{area}} \text{ and } l_1/l_2 \ge T_l \\ \text{others}, & \text{otherwise} \end{cases} \quad (2)$$

where $A(\cdot)$ is the area operator, $A(\mathcal{C}_i)$ represents the area of region $\mathcal{C}_i$. Threshold T_l is set to 4 empirically to make sure that the epidermis is narrow and long.

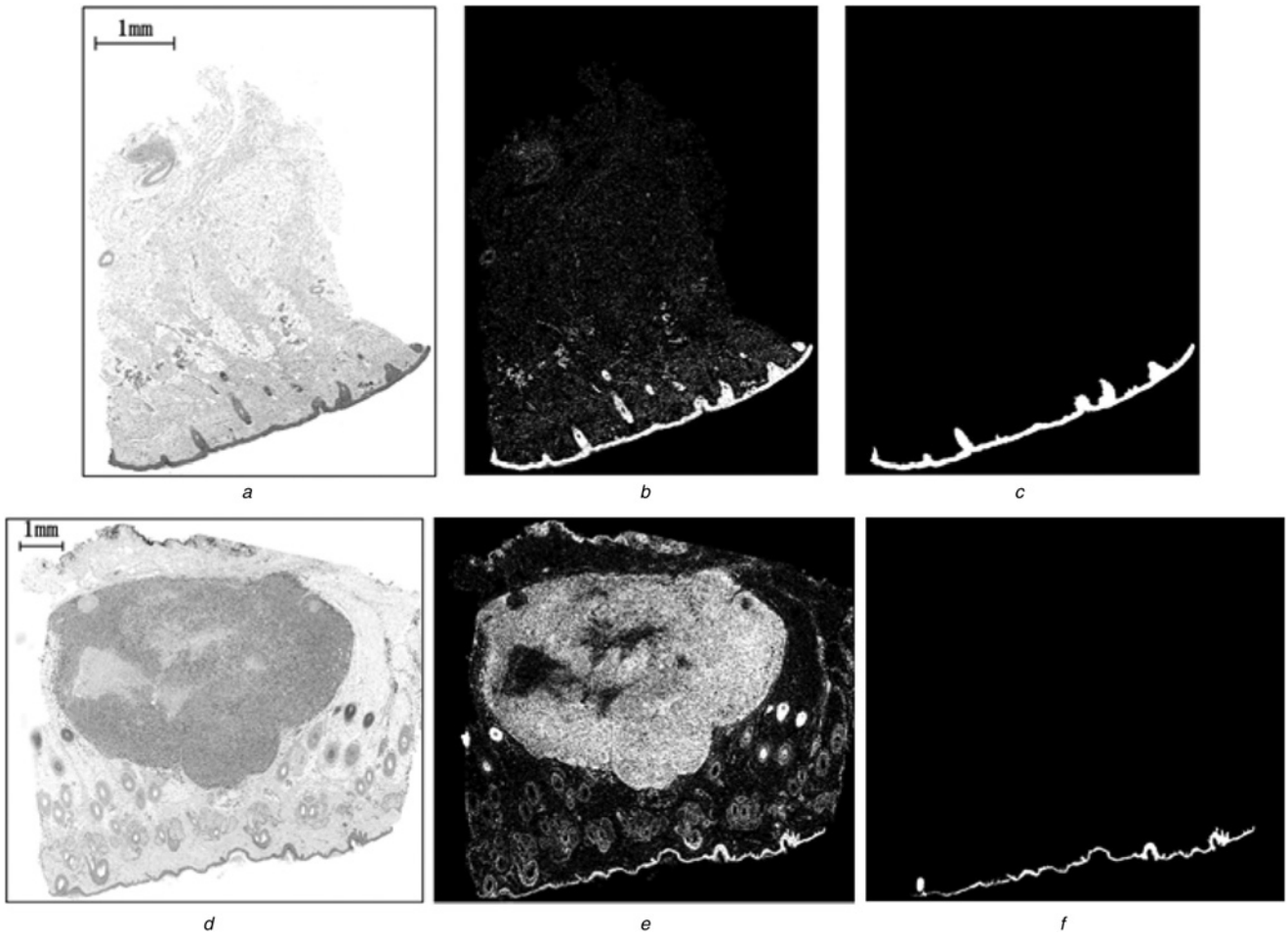

Fig. 3 *Examples of initial epidermis segmentation*

a, *d* Show original red channel image
b, *e* Show the results after global threshold
c, *f* Show the binary image after the shape analysis

After eliminating all the unrelated components, we obtain binary image B which contain the initial segmentation result. Define the proportion of initial segmentation result as

$$\boldsymbol{P}_{\text{initial}} = \frac{\mathcal{N}_e}{\mathcal{N}_a} \tag{3}$$

where $\mathcal{N}_e$ is the number of pixels belongs to the initial segmentation $\mathcal{N}_a$ is the number of pixels of the image except the white background. $\boldsymbol{P}_{\text{initial}}$ will be used for latter processing.

So far, in some cases of skin tissue where the melanocytes are not present in the dermis area, the initial segmentation provides satisfactory result (shown in Fig. 3). Note that the initial segmentation result shown in Figs. 3*c* and *f* is very close to the manually labelled area (not shown here).

However, in other cases where the melanocytes invading into the dermis area, the appearance of the dermis and epidermis area is similar to each other (especially on the boundary between the dermis and epidermis areas). This will result in inaccurate segmentation result in which more false positive regions are included. An example is shown in Fig. 4. Note that because there are many melanocytes present in the dermis area. Once the threshold is applied, the segmented image contains many false positive regions (shown as white regions in Fig. 4*d*). In Fig. 4*f*, the initial segmentation result contains false positive region (highlighted with circle) since the melanocyte regions in dermis connected to the epidermis area.

To address the above-mentioned problem and obtain more accurate result, we propose to use a TM followed by PDF analysis method which will be discussed in the next section.

2.2 Template matching with auto-generated template

TM technique is a widely used technique for pattern detection in medical imaging [18, 19]. To improve the segmentation performance, we propose a TM technique on the red channel image, in which the template is generated automatically. The purpose of using TM technique is to enhance the signal on epidermis area and to reduce the signal on other area.

On the basis of the initial segmentation result, a template is created for the TM. The shape of the template is designed as a circle to ensure the template can be included inside the epidermis area. The centre of the template is in the middle, and the radius of the template is 3 pixels (Fig. 5 shows the designed template, where m represents the intensity of the template. The size of template is denoted as T_{wsize}, that is, $T_{\text{wsize}} = 7 \times 7$ in Fig. 5). The intensity of the template is adaptively chosen as the average intensity value of the initial segmentation result (denote it as m). Therefore for different skin slides, we have different template's intensity value.

In the TM implementation, the template is sliding on the red channel image, the response value is calculated by using the normalised cross-correlation [20], which is defined as follows

$$\gamma(u,\ v) = \frac{\sum_{x,y} I_Z(x,\ y) t_Z(x-u,\ y-v)}{\left[\sum_{x,y} I_Z(x,\ y)^2 \cdot \sum_{x,y} t_Z(x-u,\ y-v)^2\right]^{1/2}} \tag{4}$$

$$I_Z(x,\ y) = I(x,\ y) - \bar{I}_{u,v} \tag{5}$$

$$t_Z(x-u,\ y-v) = t(x-u,\ y-v) - \bar{t} \tag{6}$$

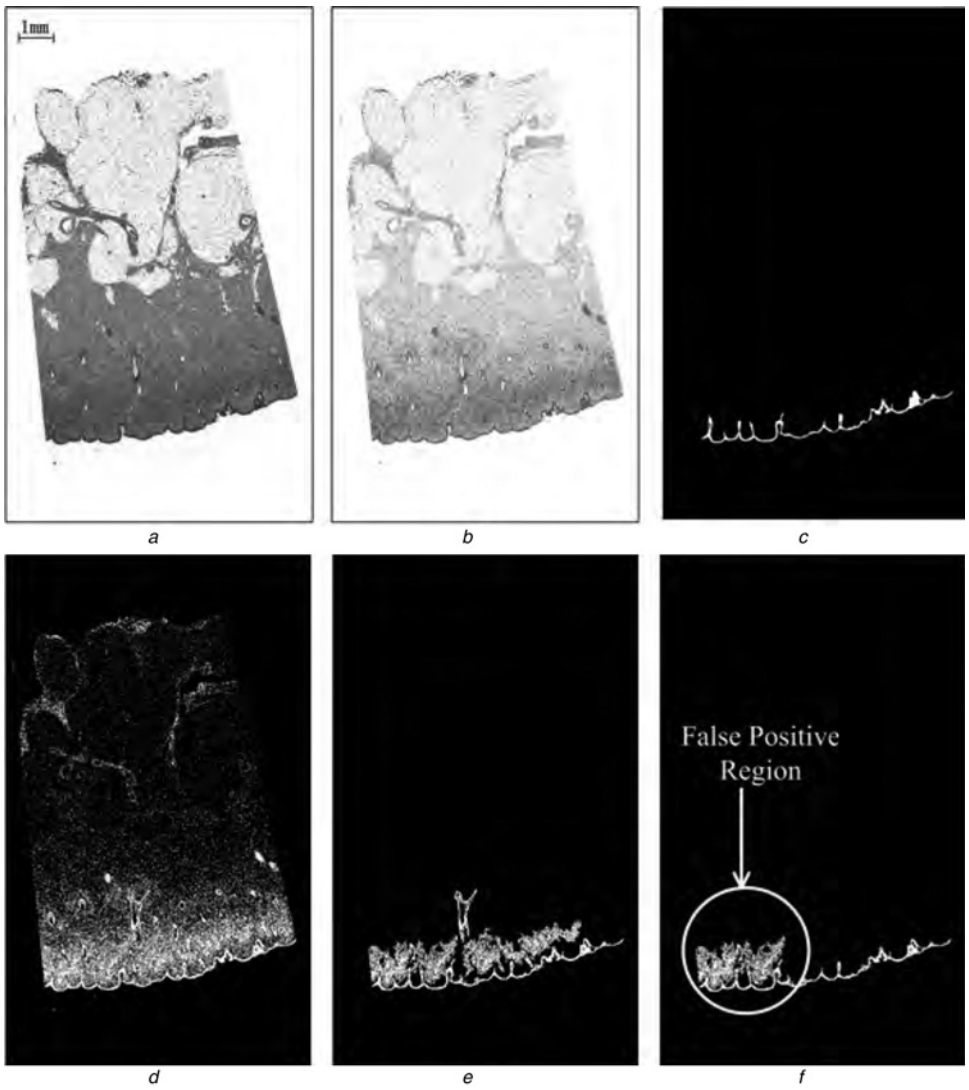

Fig. 4 *Example of initial segmentation*

a, *b* Original colour image and red channel image, respectively
c Manually labelled binary image, where white region shows the epidermis area
d Shows the binary image obtained after threshold
e Shows the binary image obtained after applying size criterion
f Shows the binary image obtained after applying the shape criterion, the false positive region is highlighted

where $I(x, y)$ is the pixel in the sub-image, (u, v) is the centre of the sub-image, $\bar{I}_{u,v}$ represents the mean of the sub-image, $t(x-u, y-v)$ is the pixel in the template and $\bar{t}$ is the mean of the template. The response value is between 0 and 1.

After the TM, we can obtain a response value image. For each pixel in the response value image, if the pixel's intensity value is close to the template's intensity value this pixel will obtain a higher response value. Otherwise, we will obtain a lower response value. In the response value image, since all the pixels inside epidermis area have similar intensity values, we can have homogenous high response value area. For the case that the melanocytes invading into the dermis area, the melanocytes may have high response values as well, however, the high response values are isolated and cannot form homogenous area. For all other areas, such as blood vessel and gland in dermis, which have different intensity values compared with the epidermis, will have lower response values. One example is shown in Fig. 6. It is shown that the epidermis area has homogenous high response value region. For the regions have invading melanocytes, we can observe many isolated high response value regions.

0	0	0	m	0	0	0
0	m	m	m	m	m	0
0	m	m	m	m	m	0
m	m	m	m	m	m	m
0	m	m	m	m	m	0
0	m	m	m	m	m	0
0	0	0	m	0	0	0

Fig. 5 *Template for TM*

2.3 PDF analysis

Once we obtain the response value image, we can now analysis the PDF of the response values in order to obtain a final global threshold for accurate epidermis segmentation.

In most cases of skin tissues, it is expected that the PDF of the response value image has two modals: one is large and another one smaller. The larger one modal is corresponding to a large

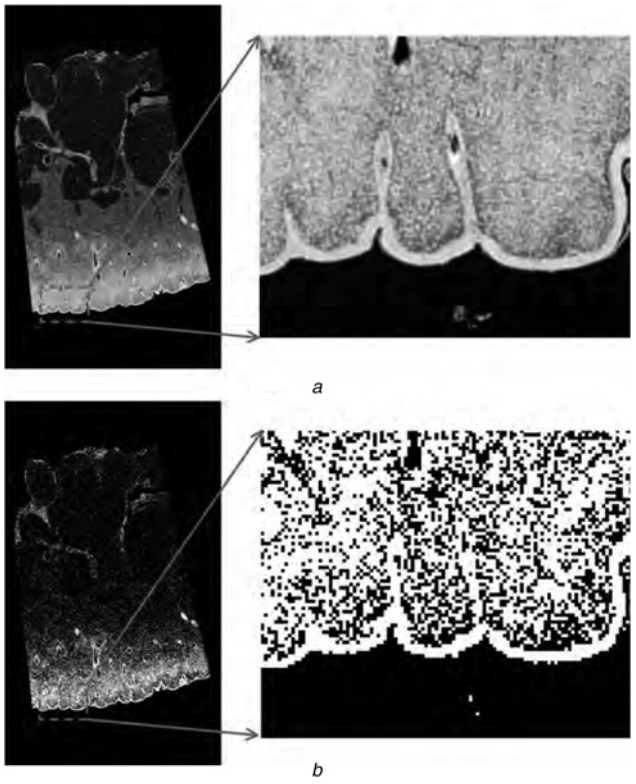

Fig. 6 *Example of the response value image*

a Lower left portion of the response value image is zoomed in for more details. The higher response value corresponds to brighter level
b Shows the same binary image in Fig. 4*d* with the zoomed in image

number of pixels belonged to unrelated regions that have lower response values. The smaller one is corresponding to the a small number of pixels belonged to the epidermis region that have higher response values. Therefore the local minimum value between the two modals can then be used for the final threshold for the response value image. However, in the case where too many melanocytes appeared in the dermis area, the PDF is not bi-modal. Two examples are shown in Fig. 7. In the case where the melanocytes are not appeared in dermis area (shown in Fig. 7*a*), it is clear that the PDF has two modals. One is centred near the lower response value area (around 0.15) which corresponds to the non-epidermis area, and another one is centred near higher response value area (around 0.5) which corresponds to the epidermis area. The minimum is highlighted in the bottom image of Fig. 7*a*, the corresponding response value can be chosen as the threshold for segmentation. In the case where too many melanocytes are appeared in dermis area (shown in Fig. 7*b*), the PDF is not bi-modal. Owing to there are many melanocytes presented in the dermis area, we have relatively large number of high response values. Therefore we can only observe one peak near the lower response value area.

Assume that the discrete response value are sampled with a step of T_{samres}, we set $T_{\text{samres}} = 0.02$ in this paper empirically. Performance with different T_{samres} are discussed in Section 3. Then we have $\delta \in [0, 0.02, 0.04, \ldots, 0.98, 1]$, where δ is a random variable. The probability of δ is defined as $P(\delta)$. On the basis of the characteristics of the PDF, we propose the following strategy to find the final threshold for the response value image segmentation:

1. Analyse if the PDF is bi-modal.
2. If the PDF is bi-modal, the minimum $P(\delta^*)$ between the two modals will be located and the corresponding response value δ^* will be used as the threshold.

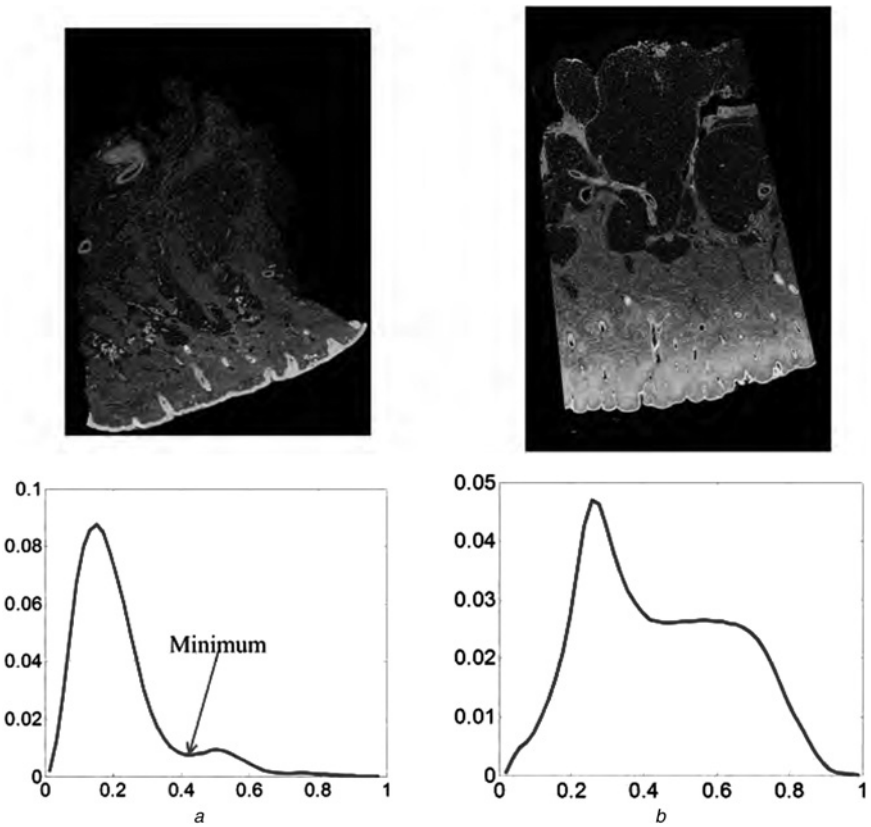

Fig. 7 *Two examples of PDF of the response value image*

a Shows the case where the melanocytes are not appeared in dermis area.
Response value image is shown on the top and its corresponding PDF is shown at the bottom
b Shows the case where the melanocytes are found in dermis area

3. If the PDF is not bi-modal, the threshold δ^* will be calculated such that it satisfies the following equation

$$\sum_{0}^{\delta^*} P(\delta) \cong 1 - \boldsymbol{P}_{\text{initial}} \tag{7}$$

The left hand size of (7) computes accumulative probability function value from 0 to δ^*. Equation (7) indicates that we are calculating the main component of the PDF from the lower value area (specifically from value 0). Note that in the case when the PDF of the response value image is non-bi-modal, the threshold is difficult to determine. We need to have some clue for how many pixels are belongs to the epidermis area, thus the initial segmented epidermis area proportion $\boldsymbol{P}_{\text{initial}}$ is utilised. However, in the non-bi-modal case, the melanocytes clusters closely connected with epidermis region introduce false positive. In other words, the region of initial segmentation result is generally larger than the ground truth epidermis region. Therefore when we try to look up the epidermis, the initial segmentation result can be used as upper bound for the epidermis area. In (7), we utilise the initial segmented epidermis area proportion from (3) to constrain threshold δ^*. In other words, the threshold δ^* for current response value image is the one that makes the left hand side of (7) equal or approximately equal to the right hand side of (7).

Once we obtain the threshold δ^*, the response value image will be segment. The pixels in epidermis area have high response values, therefore the pixels greater than the threshold δ^* will be treated as epidermis area, whereas other pixels are treated as background. After the segmentation of response value image, the size and shape criterion, described in Section 2.1, are then applied again to obtain the final epidermis. Finally, the morphological opening operation with disk-like structure is applied to obtain the final segmentation result.

3 Performance evaluation

We have evaluated the proposed technique on 105 different skin WSIs. The histological sections used for image acquisition are prepared from formalin-fixed paraffin-embedded tissue blocks of skin biopsies. The sections prepared are about 4 μm thick and are stained with H&E using automated stainer. These images are captured from different skin tissue samples which contain normal 'skin', melanocytic nevus and melanoma. The distribution of the image dataset is described in Table 1. These images are captured under 40× magnification (0.24 μm/pixel) on Carl Zeiss MIRAX MIDI Scanning System (Carl Zeiss Inc., Germany). Since the sizes of the original images are large and difficult to handle, all test images are down sampled with a factor of 32. After the down sampling, all of the test images are between 2500×3000 and $6000 \times 10\,000$ pixels. Note that compared with the down sampled image, if the original image is used, the segmentation precision will not be greatly improved (we assumed that the image is under magnification of 40×). Since the epidermis is a large area that contains many nuclei, a down sampled image contains enough information (the outline of epidermis is clear even we may not find the nuclei region clearly) for the epidermis area.

The average processing time for segmenting the epidermis using the original EMBS technique, CLAHE technique and the proposed technique, for an image with 2800×3200 pixels, are about 2.64, 1.93 and 6.29 s, respectively. All experiments were running on a 2.4 GHz Intel Core II Duo central processing unit with 4 GB random access memory using MATLAB version R2011a. We also implemented the proposed technique under optimised C program language. The processing time is about 1.74 s in the C program language implementation for an image with 2800×3200 pixels.

Table 1 Description of the image dataset

Class	Number.	Percentage, %
melanoma	39	37.14
nevus	35	33.33
normal skin	31	29.52
total	105	100

Table 2 Performance evaluation of the epidermis segmentation

Technique	$\mathcal{A}_{\text{SEN}}$, %	$\mathcal{A}_{\text{SPE}}$, %	$\mathcal{A}_{\text{PRE}}$, %
EMBS	91.68	99.76	56.05
CLAHE	93.93	96.94	53.80
the proposed	95.68	99.41	93.13

The manually labelled pixel-level contour of the epidermis is treated as the ground truths for evaluation. All contours were labelled by a pathologist. For the evaluation metric computation, we define GT as the ground truth region, SEG as the segmented region obtained by the automated technique. Three area-based evaluation metrics: sensitivity ($\mathcal{A}_{\text{SEN}}$), specificity ($\mathcal{A}_{\text{SPE}}$) and precision ($\mathcal{A}_{\text{PRE}}$) are defined as follows

$$\mathcal{A}_{\text{SEN}} = \frac{|\text{GT} \bigcap \text{SEG}|}{|\text{GT}|} \times 100\% \tag{8}$$

$$\mathcal{A}_{\text{SPE}} = \frac{|\overline{\text{GT}} \bigcap \overline{\text{SEG}}|}{|\overline{\text{GT}}|} \times 100\% \tag{9}$$

$$\mathcal{A}_{\text{PRE}} = \frac{|\text{GT} \bigcap \text{SEG}|}{|\text{SEG}|} \times 100\% \tag{10}$$

where $|\cdot|$ is the cardinality operator. We also compared the segmentation result with the EMBS technique [10] and CLAHE technique [5].

The performance of the three epidermis segmentation techniques on red channel images for 105 test WSIs are shown in Table 2. It is observed that in terms of sensitivity, the EMBS, CLAHE and the proposed techniques provide similar result (91.68 and 93.93% compared with 95.68%). It indicates that all techniques are able to segment most of the epidermis area successfully. However, in terms of the precision rate, the EMBS and CLAHE techniques are only at 56.05 and 53.8%, respectively. In other words, the segmentation result obtained by the EMBS and CLAHE techniques contains many false positive areas which are not the truth epidermis area. On the other hand, the proposed technique is able to eliminate the false positive area and provides 93% precision rate, which outperforms the existing techniques.

Fig. 8 shows examples of the final segmentation results obtained by the EMBS, CLAHE and the proposed technique. It is observed that the EMBS and CLAHE techniques tend to include more false positive regions near the epidermis. The result obtained by the proposed technique is very closed to the manual labelled one.

3.1 Parameter selection

There are a few parameters involved in the proposed technique. These parameters are:

- T_{pea}: the approximate proportion of epidermis in a WSI, used to calculate T_{area} in (2);
- T_l: threshold for the shape criteria, used in (2);
- T_{wsize}: window size of the template (shown in Fig. 5); and
- T_{samres}: sampling resolution of response value, discussed in Section 2.3.

Different selection of parameters may lead to different performance. In this section, we evaluate the performance of the proposed technique with different parameter selections. Fig. 9 shows the performance of the proposed technique while tuning

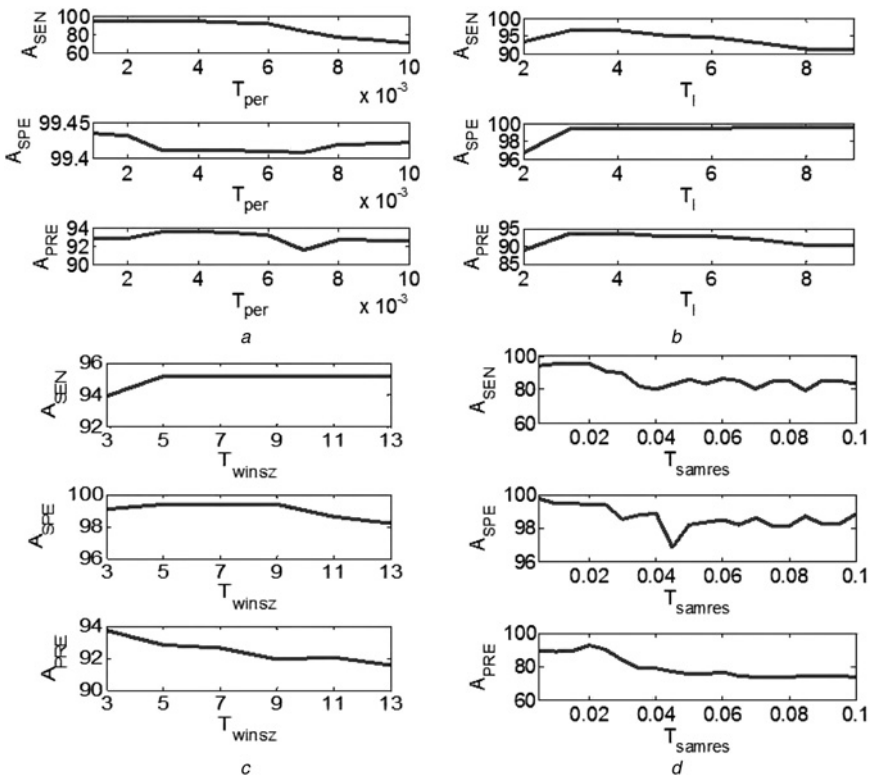

Fig. 8 *Performance evaluation for different parameter values of*

a T_{pea}
b T_l
c T_{wsize}
d T_{samres}

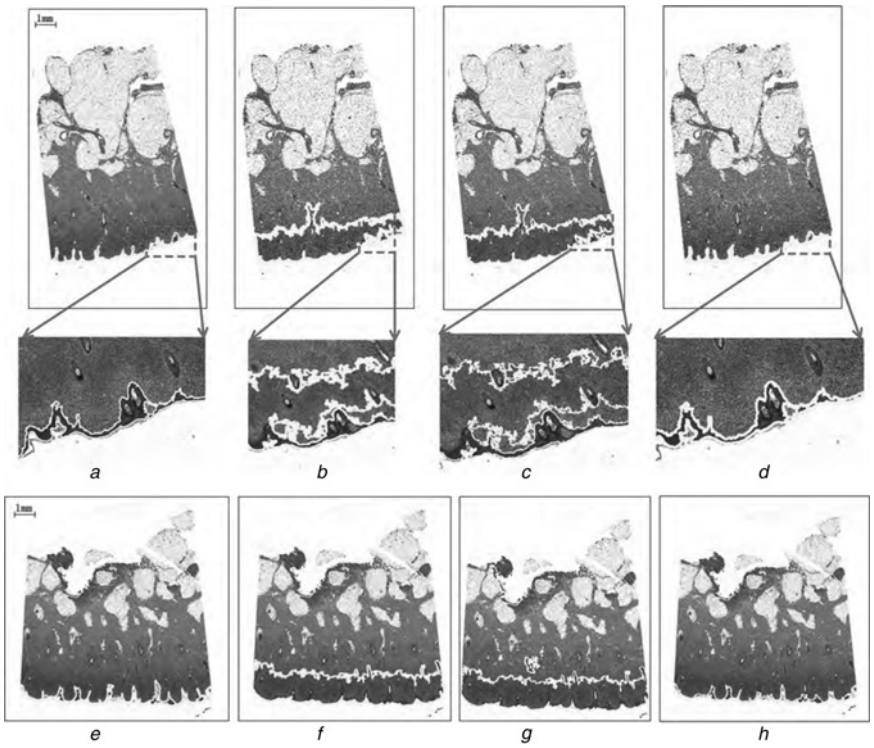

Fig. 9 *Examples of the final segmentation results*

Epidermis area contours are superimposed on the original images
a, *e* Show the segmentation result obtain by the proposed technique
b, *f* Show the segmentation result obtain by the EMBS technique [10]
c, *g* Show the segmentation result obtain by the CLAHE technique [5]
d, *h* Show the manually labelled epidermis contours

Table 3 Parameters settings for Fig. 9

Figure	Tuning parameter	Step	Other parameters setting
Fig. 9*a*	$T_{pea} = 0.001$ to 0.01	0.001	$T_I = 4$, $T_{wsize} = 7 \times 7$, $T_{samres} = 0.02$
Fig. 9*b*	$T_I = 2$–9	1	$T_{pea} = 0.004$, $T_{wsize} = 7 \times 7$, $T_{samres} = 0.02$
Fig. 9*c*	$T_{wsize} = 3 \times 3$ to 13×13	2	$T_{pea} = 0.004$, $T_I = 4$, $T_{samres} = 0.02$
Fig. 9*d*	$T_{samres} = 0.005$ to 0.1	0.005	$T_I = 4$, $T_{pea} = 0.004$, $T_I = 4$, $T_{wsize} = 7 \times 7$

four parameters mentioned above, whereas the parameter settings are listed in Table 3.

Overall, the proposed technique is able to provide satisfactory segmentation result on 105 H&E stain WSIs dataset. However, some minor issues still need to be considered in order to apply the technique in routine clinical practice. The first issue is the staining quality of the tissue slide. Owing to the uneven absorption of stain, and imperfection slide preparation procedure, the colour intensity present in WSI may vary from local regions. A possible way to reduce the influence of the colour variation is to perform the stain normalisation and equalisation [21] before applied our proposed epidermis segmentation technique. The second issue is related to the hair follicles (the 'bulges' with holes) that usually present in the epidermis area (check Fig. 1). The presence of hair follicles will affect the performance of epidermis segmentation, that is, decreasing precision rate. However, they are very difficult to exclude with automated technique. Fortunately, the presence of hair follicles will not affect the further image analysis on pre-segmented epidermis. The third issue is related to the small and often circular islands/fragments of epidermis because of the imperfect slide preparation procedure. Since the proposed technique uses shape and size criteria to filter out small regions, such isolated islands/fragments are easily to be treated as negative region and excluded from the final result. However, note that these fragments are generally small and have little contribution on further analysis. In application that requires perfect segmentation result, a post editing tool can be added after the proposed segmentation technique. Therefore that the false positive can be excluded and the missed regions can be included in the final result. Nevertheless, the proposed technique is able to provide satisfactory segmentation results for general use. Note that even though we validated the effectiveness of the proposed technique on H&E stain image, the proposed technique is not only suitable for the H&E stain slides but also suitable for other kinds of stain slides, for example, the immunohistochemical slides, since the proposed technique is not heavily relying on colour-related parameters.

4 Conclusions

This paper presents an improved technique for epidermis segmentation in skin WSI. To perform an effective segmentation, a monochromatic colour channel is first determined. The proposed technique first calculates the initial segmentation result using threshold and shape analysis. On the basis of the initial segmentation result, a TM method with circle-shape template is then applied on the red channel image to enhance the signal of epidermis. A final threshold is determined to obtain the epidermis result based on analysing the PDF of the response value image. In the evaluation of 105 skin WSIs, the proposed technique addresses the limitation of the existing technique and provides superior performance, with segmentation sensitivity at 95.68%, precision at 93.13%. The performance of the proposed technique is promising and the proposed technique can be used as a fundamental module to construct a fully automated skin histopathological image analysis system, since the epidermis is a very important observation area. Further quantitative analysis, for example, melanocytes detection in the epidermis [12, 13], is able to perform based on this paper.

5 Acknowledgments

This research is partially supported by the National Natural Science Foundation of China (grant no. 61401263) and Fundamental Research Funds for the Central Universities of China (grant no. GK201402037). Part of this manuscript has been presented at The 34th Annual International Conference of the Engineering in Medicine and Biology Society (EMBS 2012) [10].

6 References

1 Ismail, S., Colclough, A., Dinnen, J., *et al.*: 'Observer variation in histopathological diagnosis and grading of cervical intraepithelial neoplasia', *Br. Med. J.*, 1989, **298**, (6675), p. 707
2 Mccarthy, S.W., Scolyer, R.A.: 'Melanocytic lesions of the face: diagnostic pitfalls, Ann. Acad. Med., Singapore, 2004, **33**, (4), pp. 3–14
3 Brenn, T.: 'Pitfalls in the evaluation of melanocytic lesions', *Histopathology*, 2012, **60**, (5), pp. 690–705
4 Racoceanu, D., Capron, F.: 'Towards semantic-driven high-content image analysis. An operational instantiation for mitosis detection in digital histopathology', *Comput. Med. Imaging Graph.*, 2014, **42**, pp. 1–25
5 Mokhtari, M., Rezaeian, M., Gharibzadeh, S., Malekian, V.: 'Computer aided measurement of melanoma depth of invasion in microscopic images', *Micron*, 2014, **61**, pp. 40–48
6 Cruz-Roa, A., Basavanhally, A., González, F., *et al.*: 'Automatic detection of invasive ductal carcinoma in whole slide images with convolutional neural networks, March 2014, 9041, (216), p. 904103
7 Lu, C., Mandal, M.: 'Toward automatic mitotic cell detection and segmentation in multispectral histopathological images', *IEEE J. Bio. Health Info*, 2014, **18**, (2), pp. 594–605
8 Maglogiannis, I., Doukas, C.: 'Overview of advanced computer vision systems for skin lesions characterization', *IEEE Trans. Inf. Technol. Biomed.*, 2009, **13**, (5), pp. 721–733
9 Weedon, D., Strutton, G.: 'Skin pathology' (Churchill Livingstone, New York, 2002), vol. 430
10 Lu, C., Mandal, M.: 'Automated segmentation and analysis of the epidermis area in skin histopathological images'. 2012 Annual Int. Conf. of the IEEE Engineering in Medicine and Biology Society (EMBC), 2012, pp. 5355–5359
11 Lu, C., Mahmood, M., Jha, N., Mandal, M.: 'A robust automatic nuclei segmentation technique for quantitative histopathological image analysis', *Anal. Quant. Cytol. Histopathol.*, 2012, **12**, pp. 296–308
12 Lu, C., Mahmood, M., Jha, N., Mandal, M.: 'Detection of melanocytes in skin histopathological images using radial line scanning', *Pattern Recognit.*, 2013, **46**, (2), pp. 509–518
13 Lu, C., Mahmood, M., Jha, N., Mandal, M.: 'Automated segmentation of the melanocytes in skin histopathological images', *IEEE J. Biomed. Health Inf.*, 2013, **17**, pp. 284–296
14 Nielsen, P.S., Spaun, E., Riber-Hansen, R., Torben, S.: 'Automated quantification of MART1-verified Ki-67 indices: useful diagnostic aid in melanocytic lesions', *Human Pathol.*, 2014, **45**, (6), pp. 1153–1161. Available at http://www.ncbi.nlm.nih.gov/pubmed/24704158
15 Otsu, N.: 'A threshold selection method from gray-level histograms', *IEEE Trans. Syst. Man Cybern.*, 1979, **9**, (1), pp. 62–66
16 Gonzalez, R., Woods, R.: 'Digital image processing', (Wiley, New York, 2002)
17 Fitzgibbon, A.W., Pilu, M., Fisher, R.B.: 'Direct least-squares fitting of ellipses', *IEEE Trans. Pattern Anal. Mach. Intell.*, 1999, **21**, (5), pp. 476–480
18 Naik, S., Doyle, S., Agner, S., Madabhushi, A., Feldman, M., Tomaszewski, J.: 'Automated gland and nuclei segmentation for grading of prostate and breast cancer histopathology'. Proc. Fifth IEEE Int. Symp. Biomedical Imaging: From Nano to Macro ISBI 2008, 2008, pp. 284–287
19 Sintorn, I., Homman-Loudiyi, M., Söderberg-Nauclér, C., Borgefors, G.: 'A refined circular template matching method for classification of human cytomegalovirus capsids in tem images', *Comput. Methods Prog. Biomed.*, 2004, **76**, (2), pp. 95–102
20 Lewis, J.: 'Fast normalized cross-correlation'. in Vision Interface (Citeseer, Quebec City, Canada, 1995), vol. 10, pp. 120–123
21 Niethammer, M., Borland, D., Marron, J.S., *et al.*: 'Appearance normalisation of histology slides', Machine Learning in Medical Imaging, (Springer Berlin Heidelberg, 2010), pp. 58–66